Journal of Power Sources 196 (2011) 6110–6117

Contents lists available at ScienceDirect

Journal of Power Sources

journal homepage: www.elsevier.com/locate/jpowsour

Experimental investigation of current distributions in a direct methanol fuel cell with various gas diffusion layers and Nafion® membranes

Sang-Min Park[a,b], Sang-Kyung Kim[a,*], Seongyop Lim[a], Doo-Hwan Jung[a], Dong-Hyun Peck[a], Won Hi Hong[b,**]

[a] Fuel Cell Research Center, Korea Institute of Energy Research, 71-2 Jang-dong, Yuseong-gu, Daejeon 305-343, Republic of Korea
[b] Department of Chemical and Biomolecular Engineering (BK21 Program), KAIST, 335 Gwahak-ro, Yuseong-gu, Daejeon 305-701, Republic of Korea

ARTICLE INFO

Article history:
Received 21 December 2010
Received in revised form 15 March 2011
Accepted 25 March 2011
Available online 1 April 2011

Keywords:
Direct methanol fuel cell
Current distribution
Gas diffusion layer
Microporous layer
Membrane thickness

ABSTRACT

The influences of the gas diffusion layer (GDL) properties on the current distributions of a direct methanol fuel cell are investigated. Cathode GDLs with different hydrophobicity/hydrophilicity, air permeability, microporous layer (MPL), thickness, and texture properties are examined. Among the GDLs examined, a thin hydrophobic GDL with an MPL has the most homogeneous current distribution, which is primarily ascribed to the better water management capabilities of the cathode GDL properties. The differences in the current distribution among the different GDLs are more apparent when the air flow rate and loaded current are lower. The effect of the membrane thickness on the current distributions is also investigated. Among the membranes examined, Nafion® 112 has different current distributions from the others, whereas there is no noticeable difference between the current distributions with Nafion® 115 and Nafion® 117. The current distribution with Nafion® 112 is most affected by the enhanced methanol crossover and the high mixed potential.

1. Introduction

For polymer electrolyte fuel cells (PEFCs), including direct methanol fuel cells (DMFCs), many studies have experimentally or theoretically examined the spatial difference of the performance along the surface of the membrane-electrode assembly (MEA) during operation. It is important to investigate the spatial difference because the continual unevenness of spatial performance eventually diminishes the durability of PEFCs [1–3]. Measuring the current distribution using a current mapping method is recognized as a simple quantitative method to directly measure the spatial performance [1–7].

The spatial difference in the performance is essentially related to the mass transport phenomena that occur inside PEFCs. In DMFCs, two-phase flows of a liquid methanol solution and CO_2 gas in the anode side, flows of air and vapor/liquid water in the cathode side, and a methanol crossover flow from the anode side to the cathode side are representative of the mass transport phenomena. Many studies have discussed how these phenomena affect the spatial difference in DMFC performance [8]; most studies have focused on the effects of the operating conditions such as reactant feed condition, operating temperature, and flow field configurations [2,3,6,9,10].

The materials that form the MEA are the key components that determine the performance of DMFCs. The MEA is usually composed of an electrolyte membrane, catalyst layer, and electrode (gas diffusion layer, GDL). Each component should be carefully chosen and/or designed to attain high performance. As well as catalytic activity, the structure of the catalyst layer, GDL, and membrane affect cell performance. For the catalyst layer, the layer thickness, carbon support morphology, and amount of binder affect the performance [11,12]. For the GDL, the physical or chemical properties, such as texture, hydrophobicity/hydrophilicity, air permeability, and existence of a microporous layer (MPL), determine the layer structure and can affect the mass transfer that occurs inside a cell as well as cell performance [13–15]. For an electrolyte membrane, the methanol permeability and proton conductivity of the membrane, which are determined by membrane properties such the membrane thickness and chemical composition, affect cell performance [16–19]. Therefore, regarding the MEA properties in DMFCs, many studies have been undertaken to experimentally and numerically examine how these affect mass transport and cell performance [8]. However, only a few studies have reported how the MEA properties influence the spatial difference in performance during the operation of DMFCs [6].

In the present study, the effect of the differences in GDL and membrane properties on current distributions was investigated to

* Corresponding author. Tel.: +82 42 860 3366; fax: +82 42 860 3739.
** Corresponding author. Tel.: +82 42 350 3919; fax: +82 42 350 3910.
E-mail addresses: ksk@kier.re.kr (S.-K. Kim), whhong@kaist.ac.kr (W.H. Hong).

0378-7753/$ – see front matter © 2011 Elsevier B.V. All rights reserved.
doi:10.1016/j.jpowsour.2011.03.051

Table 1
GDLs (SIGRACET® GDL by SGL Technologies GmbH) examined in this study and their properties [20].

GDL	Existence of MPL	Hydrophilicity	Thickness, μm	Material
GDL 25AA	No	Hydrophilic	190	Carbon paper
GDL 25BA	No	Hydrophobic	190	Carbon paper
GDL 25BC	Yes	Hydrophobic	240	Carbon paper
GDL 10BC	Yes	Hydrophobic	420	Carbon felt

quantitatively analyze DMFC performance at each location. Based on previous results on the effect of cell operating conditions [3], the effects of the variation in texture, hydrophobicity/hydrophilicity, air permeability, existence of an MPL on the GDL, and membrane thickness on the control of the current distribution were analyzed.

2. Experimental

2.1. Preparation of the MEA

To investigate the effect of the GDL properties on the current distributions, the GDLs for the cathode electrode were varied. Four types of GDLs from the SIGRACET® GDL series (SGL Technologies GmbH) were selected for comparisons, as shown in Table 1 [20]. The four types selected represent GDLs that have carbon paper without any treatment (SIGRACET® GDL 25AA), carbon paper with hydrophobic treatment (SIGRACET® GDL 25BA), carbon paper with hydrophobic treatment and MPL (SIGRACET® GDL 25BC), and a thick carbon felt with a hydrophobic treatment and MPL (SIGRACET® GDL 10BC). Hereafter, each GDL will be referred to as GDL 25AA, GDL 25BA, GDL 25BC, and GDL 10BC, respectively. Therefore, the thickness and air permeability of the samples differ from each another due to the abovementioned differences.

To investigate the effect of the membrane thickness on the current distributions, Nafion® (Du Pont) membranes with different thicknesses were selected: Nafion® 112 (50.8 μm), Nafion® 115 (127 μm), and Nafion® 117 (177.8 μm) [16,17].

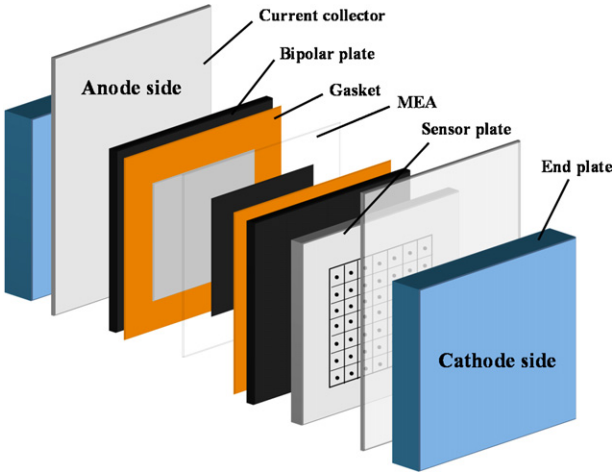

Fig. 1. Schematic of a single cell used for measurement of the current density distribution [3].

Unless otherwise specified, the GDL for the anode electrode, the cathode electrode, and the membrane were TGP-H-060 (Toray) pretreated with a 5 wt% Teflon solution, SIGRACET® GDL 25BC, and Nafion® 115, respectively.

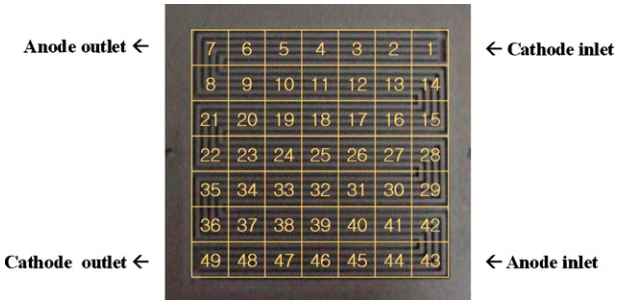

Fig. 2. Segment positions of measurement cell along the channel [3].

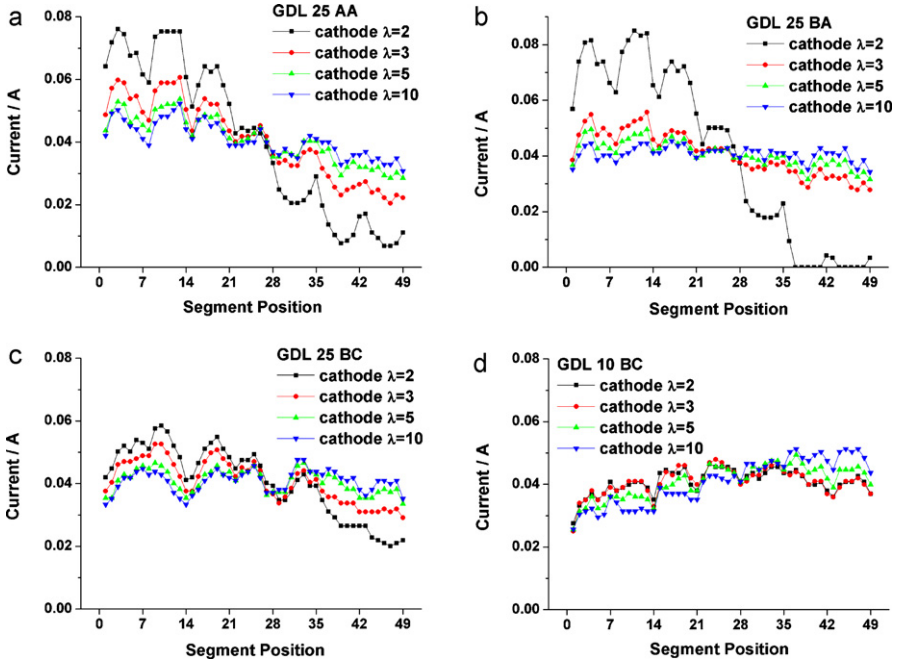

Fig. 3. Current distributions at various cathode flow rates with a current load of 2 A, with (a) GDL 25AA, (b) GDL 25BA, (c) GDL 25BC, and (d) GDL 10BC at the cathode side.

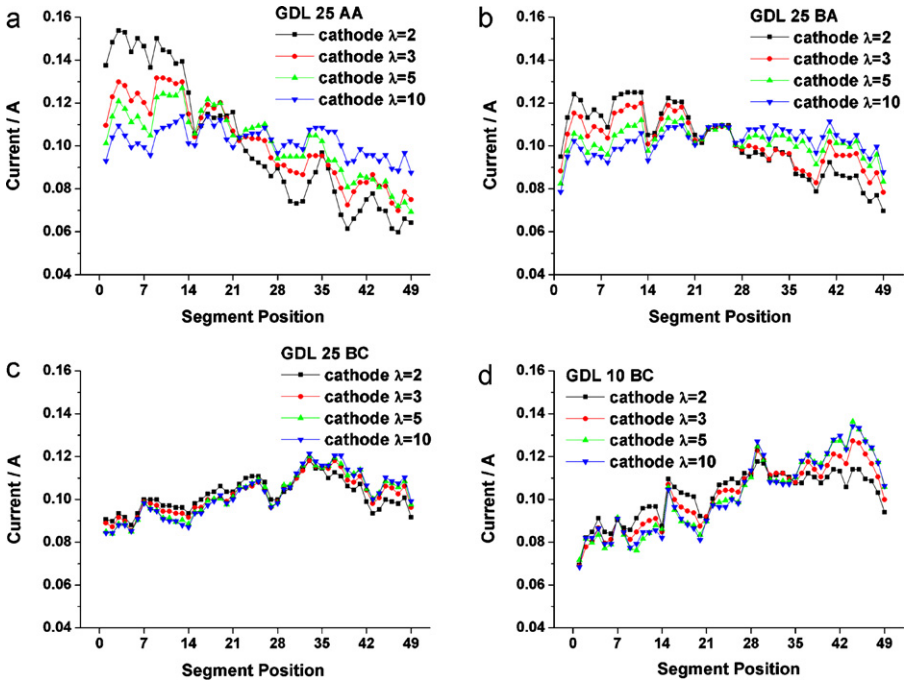

Fig. 4. Current distributions at various cathode flow rates with a current load of 5 A, with (a) GDL 25AA, (b) GDL 25BA, (c) GDL 25BC, and (d) GDL 10BC at the cathode side.

The catalysts were prepared using the same method as that described in the previous study [13]. PtRu black (HiSpec 6000™, Johnson Matthey) and Pt black (HiSpec 1000™, Johnson Matthey) were used for the anode and cathode, respectively. PtRu Black was mixed with 10 wt% of Nafion® (5 wt% Nafion® solution), and Pt Black was mixed with 7 wt% of Nafion® (5 wt% Nafion® solution) to produce the slurry for each catalyst. The amount of catalyst loading were 4 mg cm^{-2} of Pt for the anode side and 5 mg cm^{-2} of Pt for the cathode side. The Nafion® membrane was sandwiched between the two electrodes and these three components were hot pressed at 150 °C for 1 min under a pressure of 70 kgf cm^{-2}. The active area of the MEA was 25 cm^2 (5 cm × 5 cm).

2.2. Measurement of the current distribution

Current Scan Lin (S++®) was used in this study as the current mapping device (Fig. 1; [3]). The sensor plate was segmented into 49 positions, and the current density was measured at each of these segments. The five-line serpentine configuration of the flow fields, segmentation, and directions of the inlet and outlet for the reactant and the product, respectively, are also described in Fig. 2 [3].

Unless otherwise specified, the base operating conditions were as follows: galvanostatic operation mode, a total current of 2 A or 5 A on a single cell, stoichiometric factors (λ) [3] of 5 for the anode and 2–10 for the cathode, a methanol concentration of 1 M, and a cell temperature of 60 °C. The current was loaded on a single cell for 2 min while the cell voltage was measured. The current distributions and the cell voltages presented in this study represent the data obtained 100 s after the current was loaded on the single cell.

3. Results

3.1. Current distributions with different GDLs

In a previous study [3], it was found that the current densities at the cathode outlet were lowered at low air flow rates with 2 M methanol, and this is primarily a result of the water flooding caused by a lack of air and a reduced oxygen mass fraction toward the cathode outlet. However, the current distributions with 1 M methanol are more homogeneous than those with 2 M methanol under the same operating conditions. In this study, therefore, the methanol concentration was set to 1 M.

The current distributions in the MEAs with four different types of cathode GDL were measured with loaded currents of 2 A and 5 A at various flow rates. The corresponding current distributions at 2 A are presented in Fig. 3. As expected, the current distributions with hydrophobic GDLs that have an MPL (Figs. 3(c) and (d)) are comparatively homogeneous.

Except for GDL 10BC, when the air flow rate was low, the current densities near the cathode outlet were lower, and the periodical drops in current density near the U-bend were more clearly observed. For GDL 25BA in particular, the current densities near the cathode outlet showed zero values at the lowest air flow rate of λ = 2. For GDL 10BC, however, a lower current density near the cathode outlet and periodical drops were barely observed. The lowered current densities at the cathode outlet region and the periodical drops at the U-bend region were usually observed simultaneously. This was a result of the lowered air velocity and the subsequent water accumulation in those regions.

The current distributions measured at 5 A are presented in Fig. 4. Overall, the current densities were more evenly distributed compared with those at 2 A, even though the lower current densities near the cathode outlet and the periodical drops were still observed for GDL 25BA and GDL 25AA, particularly at low air flow rates. For GDL 25BC, the currents were evenly distributed regardless of the air flow rate, and the periodical drops were not observed, even at low air flow rates. However, for GDL 10BC, the increase in current densities toward the methanol inlet (i.e. the cathode outlet) became more apparent when the air flow rate increased.

Figs. 5 and 6 show the current distributions as a function of the GDL type at currents of 2 A and 5 A, respectively. (The data are rearranged with those in Figs. 3 and 4.) In Fig. 5, the differences among the various GDLs in current distribution are shown to be the largest at the lowest air flow rate (λ = 2) and become smaller as the air flow rate increases. In Fig. 6, with an air flow rate of λ = 2, the current

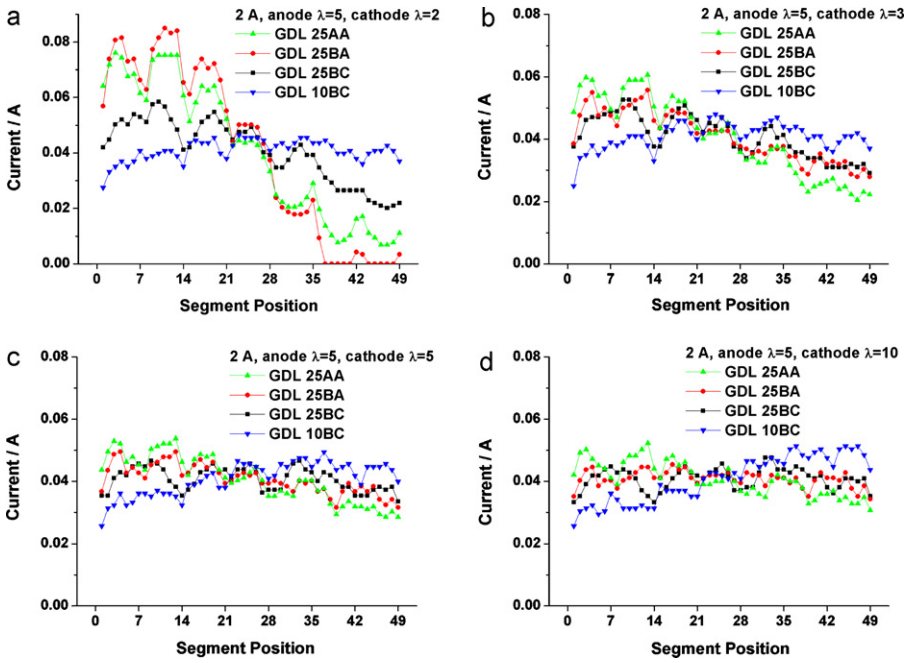

Fig. 5. Comparison of current distributions with different cathode GDLs with a current load of 2 A at different cathode flow rates (λ): (a) 2, (b) 3, (c) 5, and (d) 10.

distributions differ largely between each GDL. At 5 A, the current differences among the different GDLs are less prominent than those at 2 A.

To compare each result more clearly, plots of the cell voltages, slopes, and deviation factors are shown in Figs. 7 and 8. The slopes were determined using a linear regression from the current density data in Figs. 3 and 4. The deviation factors, called 'normalized standard deviations' in this study, are defined as the standard deviation of the current densities from the average divided by each loaded current (2 A and 5 A).

As expected, the MEA with GDL 25BC had the highest cell voltages at all air flow rates and at both loaded currents [13]. Compared with the MEA with GDL 25BC, the MEAs with GDL 25BA and GDL 25AA showed lower cell voltages due to bad water management. The MEA with GDL 10BC also showed a lower cell voltage than 25BC, especially at high air flow rates, which is a possible result of the high through-plane electrical resistance from the thick diffusion layer of GDM 10BC that leads to a high ohmic and mass transfer overpotential [21].

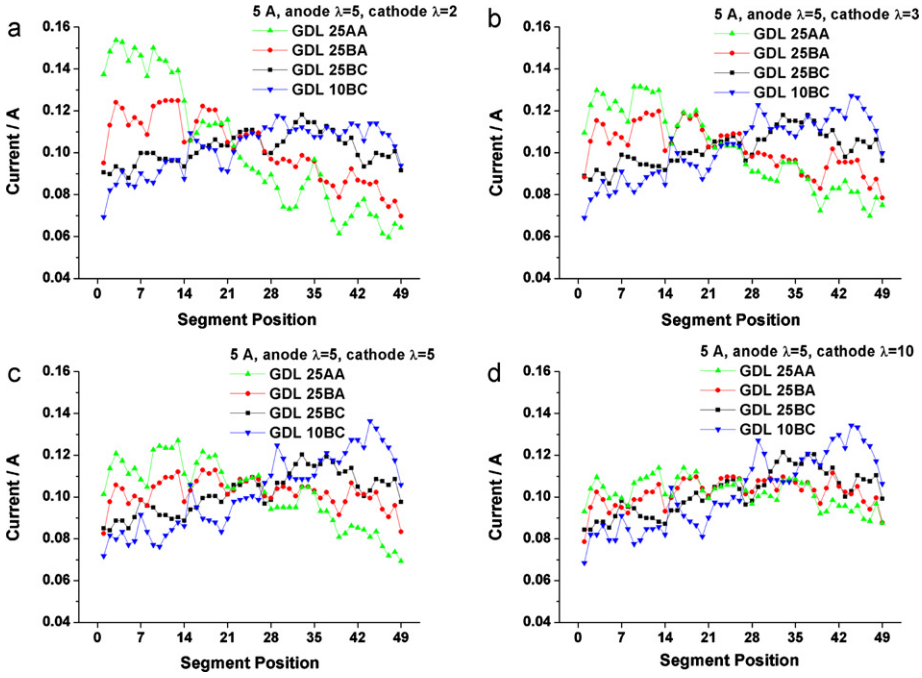

Fig. 6. Comparison of current distributions with the different cathode GDLs with a current load of 5 A at different cathode flow rates (λ): (a) 2, (b) 3, (c) 5, and (d) 10.

The slopes in Figs. 7(b) and 8(b) represent how the current densities change from the direction of the cathode inlet to that of the cathode outlet with a rough estimation of the current densities approximated as a linear change along the path. At both 2 A and 5 A, the slopes for GDL 25BA and GDL 25AA exhibited negative values at all air flow rates, whereas those for GDL 10BC showed positive values at all air flow rates.

The deviation factors in Figs. 7(c) and 8(c) represent how much the current density measured at each point deviates from the average current. At the lower current (2 A), the deviation factor decreases as the air flow rate increases for GDL 25BC, GDL 25BA, and GDL 25AA; however, for GDL 10BC only, it slightly increase as the air flow rate increases. At the higher current (5 A), the changes in the deviation factors due to an increase in the air flow rate show a similar behavior to that at 2 A. For GDL 25BC, however, the factor slightly increases as the air flow rate increases, which is a trend opposite to that displayed at 2 A [3].

3.2. Current distributions with different Nafion® membrane thicknesses

The current distributions with different membrane thicknesses were examined. For the MEAs with Nafion® 112, Nafion® 115, and Nafion® 117, the current distributions and corresponding cell voltages at various anode and cathode flow rates were measured as shown in Figs. 9 and 10. In Fig. 9, the anode flow rates were set to $\lambda = 2$ for all cases, whereas the air flow rates were varied from $\lambda = 2$ to $\lambda = 10$ to observe how the current distributions were affected by the membrane thickness at different air flow rates. To produce Fig. 10, however, the air flow rates were set to $\lambda = 2$ for all cases, after which the anode flow rates were varied. The two thicker membranes (Nafion® 117 and Nafion® 115) showed little difference in current distribution. In contrast, the MEA with the thinnest membrane (Nafion® 112) showed very different current distributions, which may have resulted from the enhanced methanol crossover through this membrane [17]. In Fig. 9 (when the anode flow rates were set to $\lambda = 2$), it is noteworthy that the MEA with Nafion® 112 had much higher current densities near the cathode outlet (i.e. anode inlet) than near the cathode inlet, whereas those with Nafion® 115 and Nafion® 117 had slightly lower current densities near the cathode outlet than near the cathode inlet or had even current distributions.

The current distributions with Nafion® 112 are presented under various flow rate conditions in Fig. 11. With Nafion® 112, there were two types of representative current distribution profiles. In the first, which represents most cases, the current densities became lower toward the cathode inlet (i.e. enhanced toward the cathode outlet). In the second, the current densities became lower toward the cathode outlet, which was apparent when the cathode flow rate was low compared with the anode flow rate (cathode $\lambda = 2$ with anode $\lambda = 5$ or 10). The former case was affected more by enhanced leakage current near the cathode inlet due to the high air flow rate from the cathode inlet [17]. The latter was affected more by reduced oxygen concentrations due to water clogging near the cathode outlet, as was discussed in a previous study [3]. With Nafion® 112, in this current region (80 mA cm^{-2}), the leakage current is primarily attributed to diffusion through the membrane rather than to electro-osmotic drag [17]. In this study, the diffusion coefficient was determined by the membrane thickness.

Another characteristic of the current distribution with Nafion® 112 is that periodical current peaks were frequently observed where the channel direction was inverted (e.g., U-bend [3,22]), simultaneously with the first type of current distribution profile described above (e.g., the current densities are lowered toward the cathode inlet). This behavior can be ascribed to the configuration of the five-line serpentine channel and the mass transport of

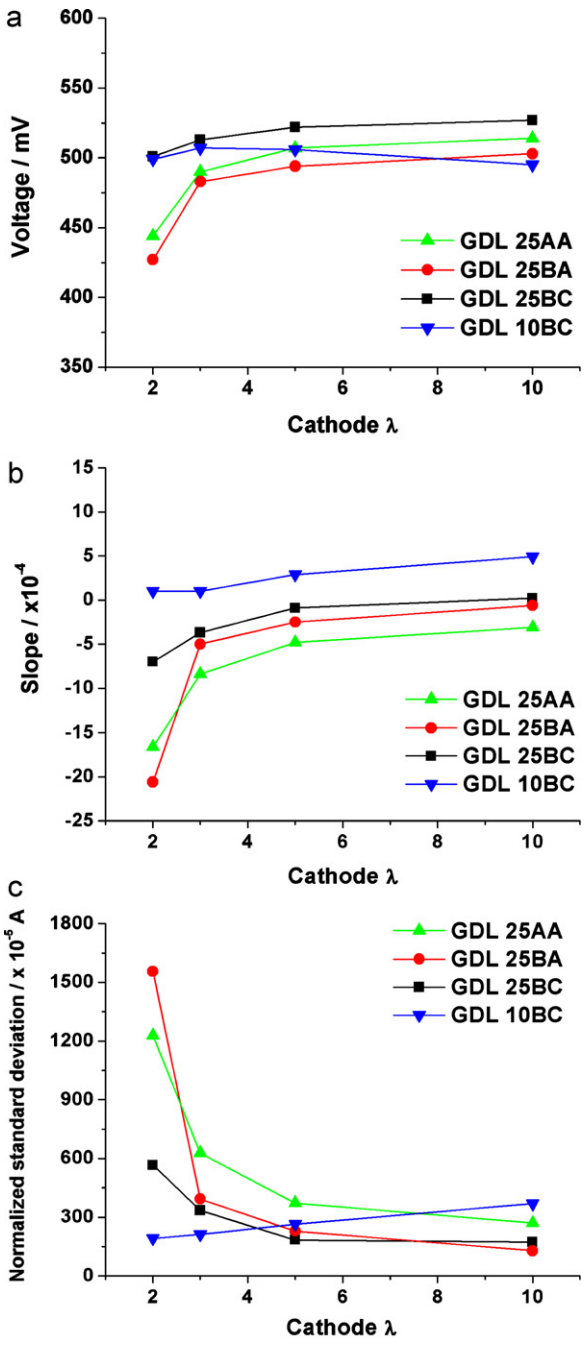

Fig. 7. Comparison of (a) cell voltages, (b) slopes, and (c) deviation factors with different cathode GDLs at various cathode flow rates and a current load of 2 A.

methanol. Where the flow direction is inverted, the current leakage by oxidation of the crossover methanol decreases because the methanol solution velocity in the anode is lower than that at other locations. Accordingly, the local reduction in the leakage current may result in a local peak in the current.

As shown in Fig. 11, when the air flow rate is relatively low compared with the anode flow rate, periodical peaks are less apparent or even disappear. Instead, a reduced current density can be observed near the cathode outlet, which was a representative phenomenon in the previous study [3]; it was observed under the conditions of a low air flow rate, high anode flow rate, and with Nafion® 115 and 2 M methanol.

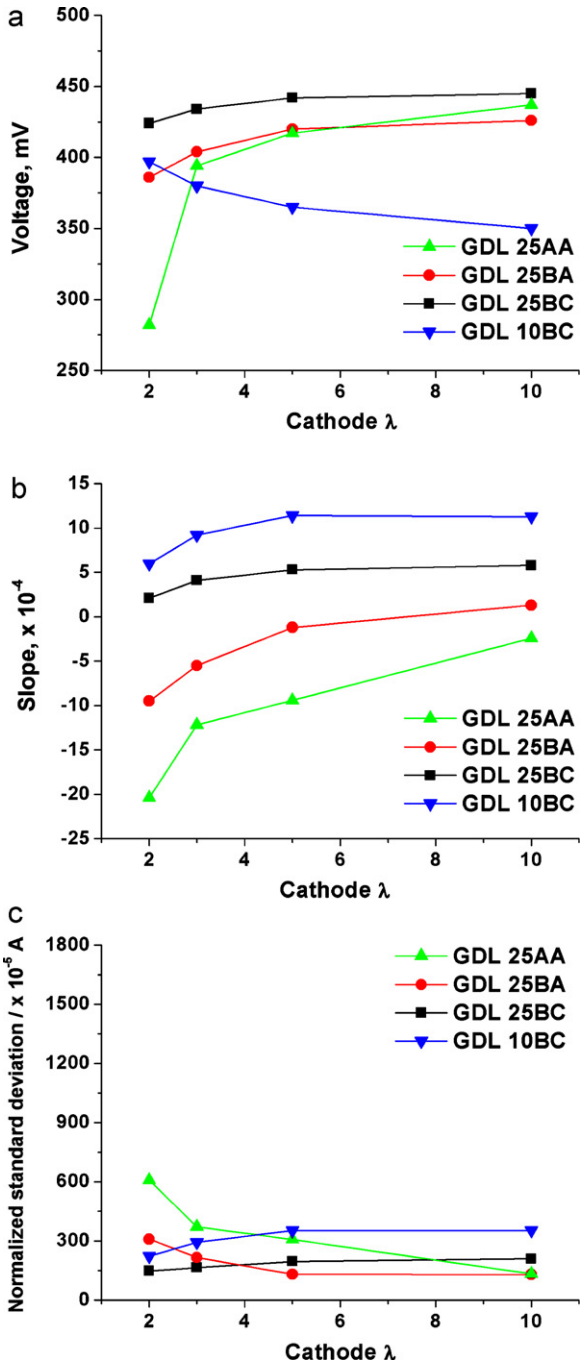

Fig. 8. Comparison of (a) cell voltages, (b) slopes, and (c) deviation factors with different cathode GDLs at various cathode flow rates and a current load of 5 A.

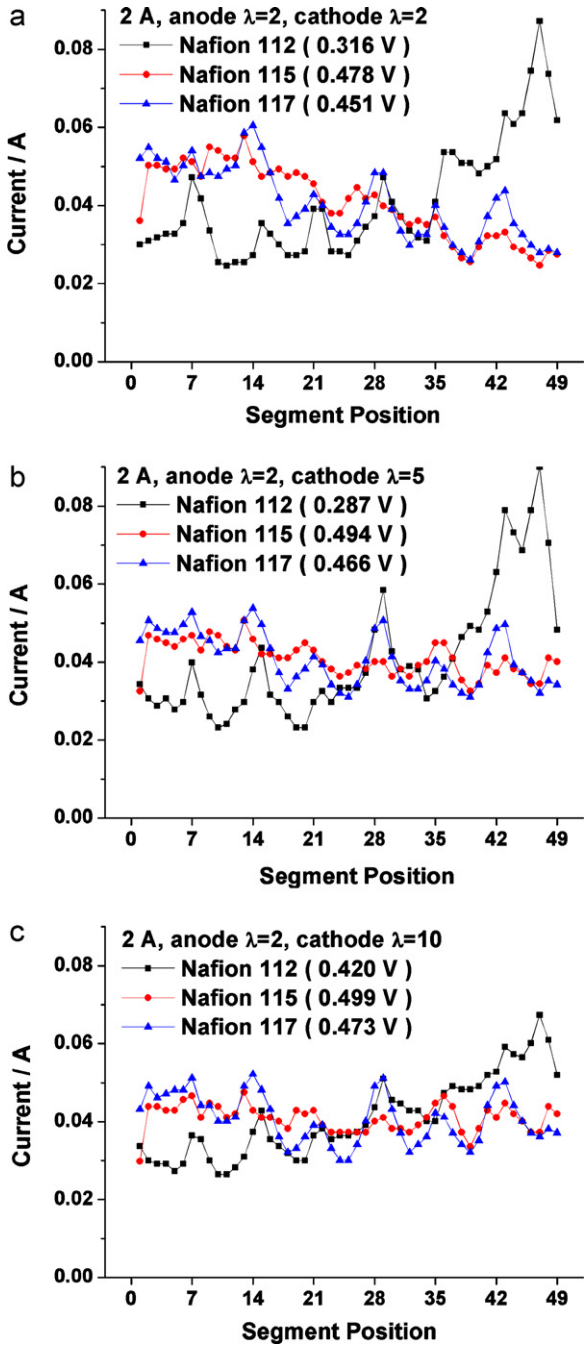

Fig. 9. Comparison of current distributions with different Nafion® membranes and a current load of 2 A at different cathode flow rates (λ): (a) 2, (b) 5, (c) 10.

4. Discussion

4.1. Effects of the GDL properties

It has been reported that the water produced from the oxygen reduction reaction at the cathode is difficult to remove, and water flooding occurs when a hydrophilic GDL is used [13–15]. Even though the GDL is hydrophobic, water flooding remains important because the water produced is pushed away from the hydrophobic GDL to the catalyst layer, which leads to water flooding in the catalyst layer region; in this regard, the existence of an MPL is beneficial. It is known that the MPL collects the water produced from the catalyst layer by capillary force and then transfers it to the channel [14,15], preventing water flooding. Therefore, as shown in Figs. 3–6, it can be said that GDL 25BA and GDL 25AA exhibit bad water management capabilities at the cathode outlet when the air flow rate is low, causing lower current densities in this region [3,13]. For the current distributions at 5 A, however, the flow rates required to meet the controlled stoichiometry (λ = 2–10) at the cathode are relatively high; thus, the reduced current densities in this region are less apparent than those at 2 A [3].

As shown in Figs. 3(c), (d) and 4(c), (d), the differences in the current distributions between GDL 25BC and GDL 10BC are barely observable with variations in the air flow rate, which result from the well-managed water removal. Thus, it can be said in this case that the reduced current near the cathode outlet due to the low

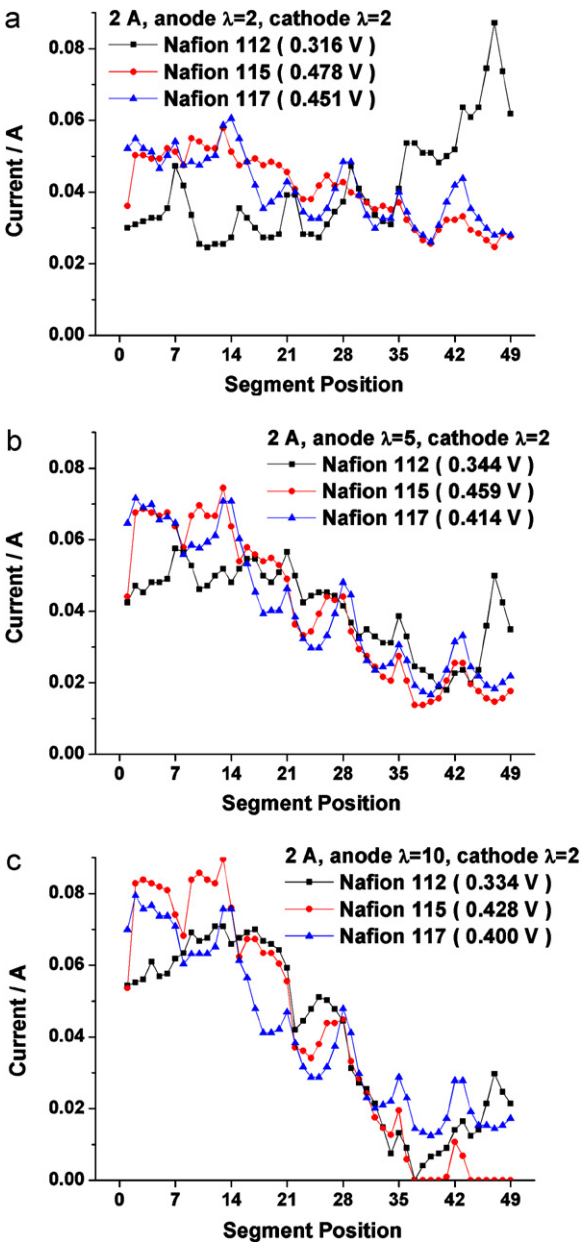

Fig. 10. Comparison of current distributions with different Nafion® membranes and a current load of 2 A at different anode flow rates (λ): (a) 2, (b) 5, (c) 10.

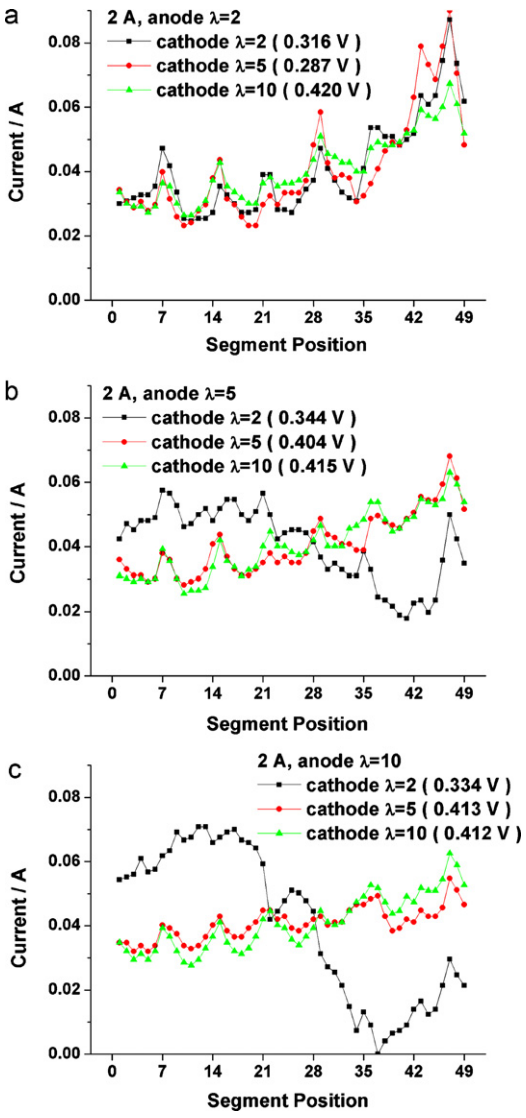

Fig. 11. Current distributions with Nafion® 112 at various cathode flow rates and a current load of 2 A at different anode flow rates (λ): (a) 2, (b) 5, (c) 10.

air flow rate and the subsequent channel clogging do not matter in this flow rate regime. In addition, by locally drying the membrane near the cathode inlet with a high air flow rate, an increase in the current distribution toward the cathode outlet can be observed [3], and this is more prominent when the air flow rate is higher.

Unlike the other GDLs, for GDL 10BC, as the cathode flow increases, the cell voltage decreases, and the deviation increases; furthermore, it is more apparent at the higher current of 5 A. For the other GDLs, the prevention of water accumulation due to removal at a higher rate of air flow may increase the current densities near the cathode outlet, as was described previously [3]. However, for GDL 10 BC, the excessively high air flow rate leads to a decrease in the cell voltage with an increase in the deviation from an even current distribution, which may be attributed to the higher air permeability of GDL 10BC. The higher air permeability of GDL 10BC with respect to that of GDL 25BC resulted from the higher porosity of the felt-type compared to the paper-type GDL [20], which, together with easy water removal due to the existence of MPL and hydrophobicity, may lead to an enhanced partial drying of the membrane near air inlet at a sufficiently high air flow rate and may then contribute to a decrease in the current density in this region. This becomes more apparent at 5 A because the air flow rates required are sufficiently high to satisfy the stoichiometric factors from 2 to 10.

4.2. *Effects of the membrane thickness*

As briefly stated in the last part of Section 3.2, it was found that the current distributions with Nafion® 112 and 1 M methanol are somewhat similar to those with Nafion® 115 and 2 M if measured under conditions of high anode flow rates and low cathode flow rates. The leakage current is relatively high under such conditions and can be affected by both membrane thickness and methanol concentration. Variation in the Nafion® thickness affects the diffusion only among the parameters that determine the leakage current, whereas variation in the methanol concentration affects both diffusion and electroosmotic drag [17]. It is concluded that, however, enhanced methanol crossover occurred due to either a thin membrane or a high methanol concentration and resulted in similar current distribution profiles. That is, even though it

was not examined directly in this study, the current distribution at a high methanol concentration (≥2 M) might be similar to distributions with a thin membrane under these flow rate conditions.

5. Conclusions

Direct methanol fuel cells that have a hydrophobic cathode GDL with a microporous layer and an electrolyte membrane of proper thickness generally exhibit relatively high performance. In this sense, the effects of GDL properties and membrane thickness on current distributions were examined. Together with the phenomena observed in the previous study [3], it was concluded that a thin hydrophobic GDL with an MPL showed the most homogeneous current distribution, and this is attributed primarily to the better water management by the GDL properties of the cathode. Furthermore, the effect of the membrane thickness on the current distributions in Nafion® 112, Nafion® 115, and Nafion® 117 were investigated. Among these, the current distributions with Nafion® 112 differed significantly from those with the other two membranes. The current distribution with Nafion® 112 appeared to be most affected by the enhanced methanol crossover.

Acknowledgement

This work was supported by New & Renewable Energy R&D program (2009T100101993) under the Ministry of Knowledge Economy, Republic of Korea.

References

[1] Z. Liu, Z. Mao, B. Wu, L. Wang, V.M. Schmidt, J. Power Sources 141 (2005) 205–210.
[2] F. Ay, A. Ata, H. Dohle, T. Sener, H. Gorgun, J. Power Sources 167 (2007) 391–397.
[3] S.-M. Park, S.-K. Kim, S. Lim, D.-H. Jung, D.-H. Peck, W.H. Hong, J. Power Sources 194 (2009) 818–823.
[4] M. Noponen, T. Mennola, M. Mikkola, T. Hottinen, P. Lund, J. Power Sources 106 (2002) 304–312.
[5] H. Sun, G. Zhang, L.-J. Guo, H. Liu, J. Power Sources 158 (2006) 326–332.
[6] V. Saarinen, O. Himanen, T. Kallio, G. Sundholm, K. Kontturi, J. Power Sources 163 (2007) 768–776.
[7] M. Mench, C.Y. Wang, J. Electrochem. Soc. 150 (2003) A79–A85.
[8] T.S. Zhao, C. Xu, R. Chen, W.W. Yang, Prog. Energy Combust. 35 (2009) 275–292.
[9] M.S. Hyun, S.-K. Kim, D. Jung, B. Lee, D. Peck, T. Kim, Y. Shul, J. Power Sources 157 (2006) 875–885.
[10] V. Saarinen, O. Himanen, T. Kallio, G. Sundholm, K. Kontturi, J. Power Sources 172 (2007) 805–815.
[11] C. Lim, R.G. Allen, K. Scott, J. Power Sources 161 (2006) 11–18.
[12] S.-M. Park, D.-H. Jung, S.-K. Kim, S. Lim, D. Peck, W.H. Hong, Electrochim. Acta 54 (2009) 3066–3072.
[13] H. Nakajima, T. Konomi, T. Kitahara, J. Power Sources 171 (2007) 457–463.
[14] A.Z. Weber, J. Newman, J. Electrochem. Soc. 152 (4) (2005) A677–A688.
[15] H.K. Atiyeh, K. Karan, B. Peppley, A. Phoenix, E. Halliop, J. Pharoah, J. Power Sources 170 (2007) 111–121.
[16] J.-Y. Park, J.-H. Lee, S.K. Kang, J.-H. Sauk, I. Song, J. Power Sources 178 (2008) 181–187.
[17] S. Eccarius, B.L. Garcia, C. Hebling, J.W. Weidner, J. Power Sources 179 (2008) 723–733.
[18] J.G. Liu, T.S. Zhao, Z.X. Liang, R. Chen, J. Power Sources 153 (2006) 61–67.
[19] V. Neburchilov, J. Martin, H. Wang, J. Zhang, J. Power Sources 169 (2007) 221–238.
[20] http://www.sglcarbon.com.
[21] L. Cindrella, A.M. Kannan, J.F. Lin, K. Saminathan, Y. Ho, C.W. Lin, J. Wertz, J. Power Sources 194 (2009) 146–160.
[22] C. Xu, T.S. Zhao, Electrochem. Commun. 9 (2007) 497–503.